Available online at www.CivileJournal.org

Civil Engineering Journal

(E-ISSN: 2476-3055; ISSN: 2676-6957)

Vol. 8, No. 06, June, 2022

Shear Strengthening of Reinforced Concrete Beam Using Wire Mesh–Epoxy Composite

Mustafa Al-Bazoon [1*], Abdulkhaliq Jaafer [1], Haidar Haidar [1], Abbas Dawood [1]

[1] *Department of Civil Engineering, College of Engineering, University of Misan, Maysan, Iraq.*

Received 26 February 2022; Revised 20 May 2022; Accepted 26 May 2022; Published 01 June 2022

Abstract

This experimental research aims to study the use of wire mesh–epoxy composite (WMEC) as a shear-strengthening technique for reinforced concrete (RC) beams by focusing on the following parameters: (1) presence of shear reinforcement in the shear span; (2) type of strengthening technique (U-jacketing, vertical U strip, or inclined strip); and (3) number of wire mesh layers (three or six layers). Nine simply supported rectangular RC beams were tested under two monotonic point loads. The testing specimens were divided into two groups: (1) five beams without shear reinforcement and (2) four beams with shear reinforcement. Load–deflection relationship, shear ductility index, beams' stiffness, energy absorption, crack propagation, mode of failure, and strain were studied for all testing specimens and compared with those of the control beams to measure the improvement from WMEC addition. Results showed that all WMEC types enhanced the shear capacity. Among the three shear-strengthening types, the continuous U-jacket scheme had a higher effect, increasing the shear capacity between 33.4 and 95.9% and the shear ductility index by 23% relative to those of the reference specimens. The shear capacity improvement by WMEC for the beams without shear steel reinforcement was greater than that for the beams with shear reinforcement under the same shear-strengthening configuration. When the number of wire mesh layers was doubled, the ultimate load was further increased from 33.4 to 57.8%. This research showed that WMEC is a practical and excellent shear-strengthening technique for RC beams.

Keywords: Shear Strengthening; Epoxy; Wire Mesh; RC Beam; Ferrocement; Jacketing.

1. Introduction

One of the major challenges of the construction industry is the rehabilitation and repair of existing structures, especially for structural members suffering from shear deficiency. The shear failure of reinforced concrete (RC) beams occurs abruptly and therefore has a catastrophic effect. The major reasons for repairing and upgrading existing structures are to extend their structural life when they approach the end of their service lives or as a result of usage change, damage due to severe environmental effects (i.e., thawing and freezing fire impairment, corrosion, and erosion), and earthquakes. The main purpose of strengthening techniques is to increase the bending and shear capacity of structural members and to control the progress of cracks and deformations.

The basic concept in the design of RC beams is flexural failure; that is, the tensile steel reinforcement reaches the yield strain before the concrete in the compression zone reaches the crushing stage. This type of failure gives an alarm before the collapse takes place. However, shear failure happens in a brittle manner and therefore should be avoided. Shear strengthening becomes a necessity when the shear strength of the RC beams is reduced for the above reasons or when the shear capacity is lower than the flexural capacity after flexural strengthening. The selection of appropriate materials and strengthening techniques depends on several factors, such as the easiness of application and time required, the skill of available human resources, and the overall cost of the strengthening process [1].

* Corresponding author: mustafa-jasim@uomisan.edu.iq

http://dx.doi.org/10.28991/CEJ-2022-08-06-09

Externally bonded reinforcement (EBR) is considered one of the most important techniques that has been utilized in retrofitting concrete members. Different EBR methods, such as steel sheets and fiber-reinforced polymer (FRP), have been investigated and have their own advantages and disadvantages. Attaching steel plates to the concrete beams' web increases the shear capacity of existing structures [2, 3]. However, rust and corrosion and difficulty in installing steel plates remain the major disadvantages of these techniques [4]. FRP considerably enhances the bending and shear capacity of RC members [5-7] and has outstanding physical and mechanical properties such as high tensile strength to weight ratio as well as its non-corrosive nature. FRB is a good solution for strengthening/rehabilitating existing RC structures instead of conventional steel materials to overcome steel plate abuses. Many experimental and numerical studies on improving the flexural and/or shear capacity of RC beams using FRB materials have been conducted. However, a major drawback of FRB is its premature debonding failure [8–10]. Moreover, the manufactured fibers are unsafe for human health because they emit airborne respirable fibers during manufacturing, utilization, and waste processing [11]. To solve the premature debonding issue, researchers applied FRP in grooves on the concrete cover and bonded it with cementitious epoxy or grout. This technique is called near-surface mounted (NSM) reinforcement [12-14]. The mechanical properties of the FRP, the depth and width of the grooves, and the preparation of the concrete surface have an effect on the performance of the NSM-FRP system [15-17]. The NSM technique is difficult to use when the concrete cover is spalled due to deteriorated or damaged concrete structures. Thus, constructing a new concrete cover exhibiting good bonding strength with the member's substrate is difficult, sometimes impossible, and requires curing and additional time to reach the maximum concrete strength. The cost of FRP is another constraint for the composite.

A recent trend in the shear strengthening of RC beams is the direct application of fiber cementitious matrix to concrete surfaces, such as high-performance fiber-reinforced composites (HPFRCs). The most common kinds of HPFRC are slurry infiltrated fiber concrete (SIFCON) and fabric-reinforced cementitious matrix (FRCM). SIFCON composite consists of short steel fibers embedded in low-viscosity cementitious slurry. The typical ratio of fiber used in SIFCON ranges from 8% to 12% by volume, and the compressive strength ranges from 80 MPa to 200 MPa [18]. Al-Rousan and Shannag [18] tested SIFCON jackets for the shear strengthening of RC beams by studying the parameters of shear-span-to-depth ratio and longitudinal reinforcement percentage and found that jacketing the members with SIFCON as external reinforcement increased the ultimate shear strength up to 53% and precluded the brittle shear failure. Meda et al. [19] studied a high-performance fiber-reinforced cementitious composite jacketing for strengthening beam defects in shear; the jacketed beams displayed an excellent shear resistance and reached their flexural capacity compared with the control specimens. Several researchers also studied the use of textile-reinforced mortar or FRCM [20-22]. The following configurations are commonly performed for strengthening: (1) side-bonded strip [23-25], (2) spaced at the distance or discontinuous U-jacketing [26-28], and (3) enclosed wrapping [29-31]. Although enclosing wrapping is an effective strengthening technique in practice, it cannot constantly be used on RC beams cast with a slab [32]. In addition, the structural performance of the strengthened members changes the failure mode from shear to flexural when multilayers of textile and mortar are used [33-35]. These systems can also address the problems relating to moisture and fire resistance. Steel-reinforced grout (SRG) is a recently developed composite system composed of galvanized steel textiles with ultrahigh strength that are twisted into ropes, collected into unidirectional textures, and inserted in an inorganic cement-based matrix. For the prevention of rusting, the steel wires are prepared using stainless steel or usually coated with zinc or brass [36]. Gonzalez-Libreros et al. [37] investigated the effect of internal steel stirrups and SRG configurations on the performance of RC beams with defective shear and found that SRG strengthening improved the beams' overall capacity by more than 30%. Ombres & Verre [38] demonstrated that the effectiveness of SRG strengthening systems was controlled by slippage at the interface of the concrete–SRG and/or steel fabric–mortar.

As a composite material (consisting of different layers of wire mesh embedded in cement mortar), ferrocement is utilized for the rehabilitation, repairing, and strengthening of different RC members. Owing to the low flexural strength of cement mortar, the flexural strength of ferrocement laminate is entirely from the wire mesh, which has a ductile behavior. Ferrocement is a low-cost material because of the availability of its raw materials and its fabrication in intricate geometries. Moreover, it exhibits a high tensile-strength-to-weight ratio and good cracking control. However, the main problems associated with the use of ferrocement as a strengthening material are its poor durability due to fine mesh corrosion, low-performance mortars, and separation of ferrocement laminate from the member soffit [39-40]. In addition, strengthening using ferrocement requires a long time to allow the mortar to reach its maximum strength (i.e., 28 days). Therefore, structural engineers are exploring new materials and/or techniques that do not require a long processing time during construction and curing stages. To solve the above problem, Yan (2015) [41] introduced a steel mesh-reinforced resin concrete (SMRC) instead of cement mortar as a new material in traditional ferrocement for the flexural strengthening of concrete beams and found that the resin concrete can reach about 80% of its ultimate strength within 24 hours.

Li et al. [42] investigated the use of SMRC for strengthened RC compression members and confirmed the efficiency of resin concrete as a rapid bonding layer. Qeshta et al. [43, 44] developed another method of replacing the cement mortar in ferrocement with an epoxy resin for the flexural strengthening of plain and RC beams. These studies showed that the combination of epoxy with steel mesh can also be used as an effective material for rapid strengthening. Jaafer et al. in 2019 [45] employed a wire mesh–epoxy composite (WMEC) to strengthen concrete slabs. Al Nuaimi et al. in

2020 [46] studied the durability of using a wire mesh–epoxy system as a strengthening material for RC members. These reports implied that the system is durable and can be an alternative material for strengthening and retrofitting RC beams under severe environmental conditions. Abadel [47] studied the use of NSM, carbon fiber-reinforced polymer, welded wire mesh, and textile-reinforced epoxy mortar to enhance the shear capacity of RC beams. However, no report is available on the use of WMEC for the shear strengthening of RC beams. U-shape jacketing, vertical strips, and inclined strips were found to improve the shear capacity to 47–56% and change the mode of failure from brittle (shear) to ductile (flexural).

Although epoxy resin requires specific environmental conditions, the main advantages of using a composite of steel wires with epoxy adhesive as a strengthening material are as follows:

- The installation process is easy, fast, and does not require curing.
- The epoxy adhesive does not occupy space because it is thin.
- WMEC is durable and has good corrosion resistance.
- WMEC does not require a framework (i.e., it can be prepared in advance).

The limitations of using epoxy mortar as an adhesive material are as follows:

- Epoxy has a relatively low thermal capacity especially when the temperature exceeds 60˚C [20].
- According to the manufacturer's recommendations, epoxy (Sikadur-31) must not be applied to wet or moisture substrates.

Using wire mesh with epoxy mortar as a strengthening technique for plain concrete beams, RC beams, punching shear for RC slabs, and confining RC columns shows it effectively improves the structural behavior of those elements. However, to the best of the authors' knowledge, the use of WMEC as a shear-strengthening technique for RC beams has not been done. Therefore, further studies are needed to understand the behavior of concrete beams under shear defects and the influence of some parameters on the ultimate shear capacity and failure mode of the strengthened beam using this technique. The main goal of the present work is to assess the effectiveness of using WMEC for the shear strengthening of RC beams. In addition, the effect of stirrups with different schemes of wire mesh–epoxy layers as external reinforcement on the shear resistance of RC beams was investigated. Nine RC beams with the same cross-section of 150×300 mm and total length of 2300 mm were fabricated and tested under monotonic load up to failure. The ultimate load capacity, stiffness, energy absorption, cracking load, and failure mode of the specimens were recorded and discussed.

2. Experimental Program

2.1. Material Properties

2.1.1. Concrete

Natural sand and gravel were used in the concrete mixture. The gradient of the sand and gravel are confirmed with the ASTM C33/03 [48]. Figures 1 and 2 show the gradient of the used sand and gravel.

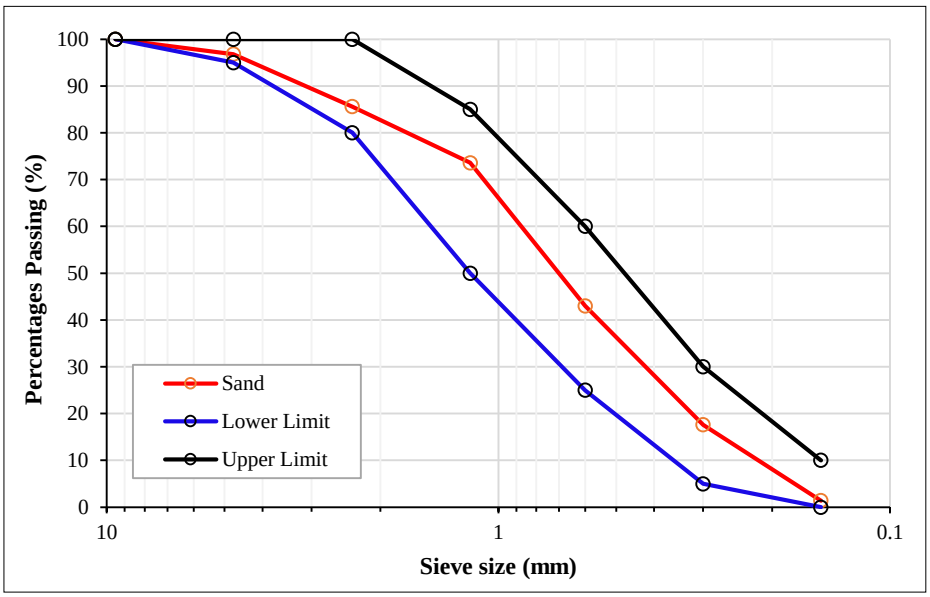

Figure 1. Sieve analysis of used sand

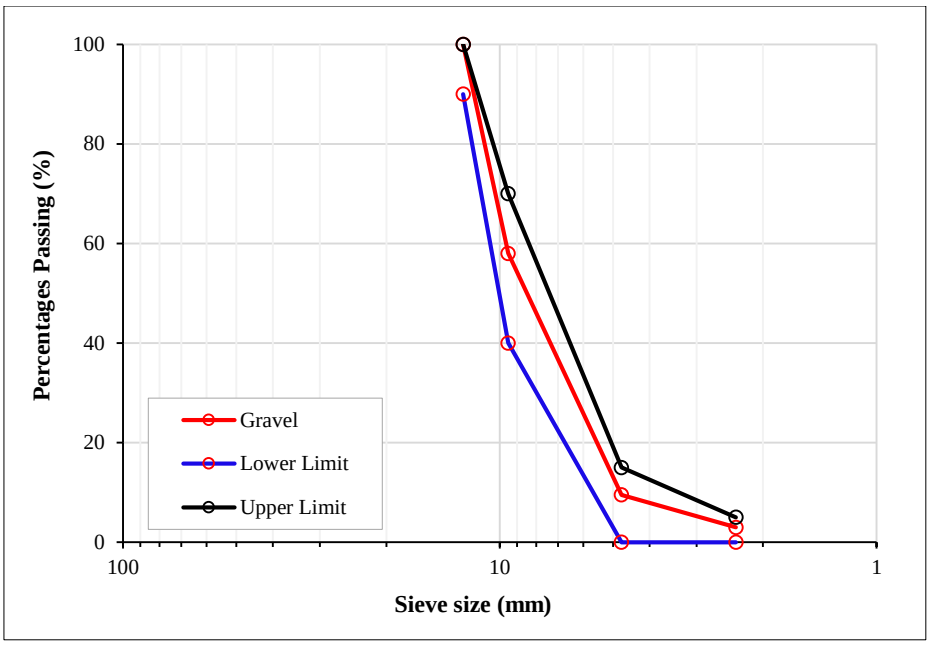

Figure 2. Sieve analysis of used gravel

All specimens were cast using one concrete batch with a target concrete compressive strength of 25 MPa. The mechanical properties of the concrete were tested after 28 days according to BS1881: Part 16:1983 [49]. The average compressive strength of the six concrete cubes (150×150×150 mm) was 25.1 MPa, the average flexural strength of six concrete prisms (100×100×500 mm) was 3.5 MPa, and the average splitting tensile strength of six concrete cylinders (150×300 mm) was 1.9 MPa. The tests were performed in accordance with the concrete testing requirements [50, 51].

2.1.2. Steel

Three types of steel reinforcement bars were used. Two steel bars of 16 mm diameter were employed as longitudinal flexural reinforcement with a concrete cover of 25 mm. The beam reinforcement ratio was $\rho = 1.0\%$. Two steel bars of 10 mm diameter were placed in the compression zone to hang the stirrups. Mildly deformed steel bars with a diameter of 6 mm were used as shear reinforcement. The mechanical properties of the steel bars in this study were determined using a standard direct tensile test (see Table 1). The elasticity modulus of all the tested steel reinforcements was 200 GPa.

Table 1. Mechanical properties of reinforcing steel

Bar size (mm)	Test results			ASTM A615M [52]		
	Yield Stress (MPa)	Ultimate Strength (MPa)	Elongation (%)	Yield Stress (MPa)	Ultimate Strength (MPa)	Elongation (%)
6	317	657.0	13.9	420	620	9
10	521	654.4	13.8	420	620	9
16	529	658.7	14.2	420	620	9

2.1.2. Welded Wire Mesh

A locally available welded steel mesh with a square opening of 10×10 mm spacing and an average wire diameter of 0.7 mm was used. Three coupons were prepared in accordance with ACI 549.1 R88 [53] to obtain the mechanical properties of the wire mesh. The average yield strength, ultimate strength, and elastic modulus were 250, 560, and 110 GPa, respectively.

2.1.3. Epoxy

A two-component thixotropic epoxy adhesive named "Sikadur-31 CF Slow" that hardens without shrinkage was used to fabricate the WMEC. According to the technical data sheet provided by the manufacturer, after 7 days of curing at 20 °C, the epoxy adhesive will have tensile adhesion strength greater than 4 MPa, tensile strength of 13 MPa, compressive strength of 54 MPa, flexural strength of 27 MPa, and elastic modulus of about 2600 MPa.

2.2. Description of Beam Specimens and Test Variables

The shear performance of simply supported beams after strengthening with external WMEC was evaluated. Nine RC beams with an overall length of 2300 mm and a clear span of 2000 mm were cast. Dimensions and longitudinal reinforcement were similar for all the specimens. The beams with a rectangular cross-section of 150 x 300 mm and 25 mm clear concrete covers on all four sides were designed as per ACI Code 318 [54] to guarantee shear failure. According to this design, the flexural (longitudinal) reinforcement consists of two steel rebars of 16 mm in diameter (d=261 mm, $\rho = 1.0\%$) placed at the bottom. Two rebars with a diameter of 10 mm were placed on top of the beam and used as stirrups' hangers. The shear span was equal to 550 mm and remained constant for all the tested specimens.

The beams were divided into two groups according to the amount of internal shear reinforcement. The first group (group S) included five beams reinforced with a closed stirrup of 6 mm in diameter, and a spacing of 130 mm was used along the shear span. The arrangement of the longitudinal and transverse reinforcement of this group is illustrated in Figure 3-a. The second group (group W) consisted of four beams without any shear reinforcement except those placed on both beam ends as shown in Figure 3-b. One beam from each group did not receive WMEC strengthening and was labeled as a reference specimen.

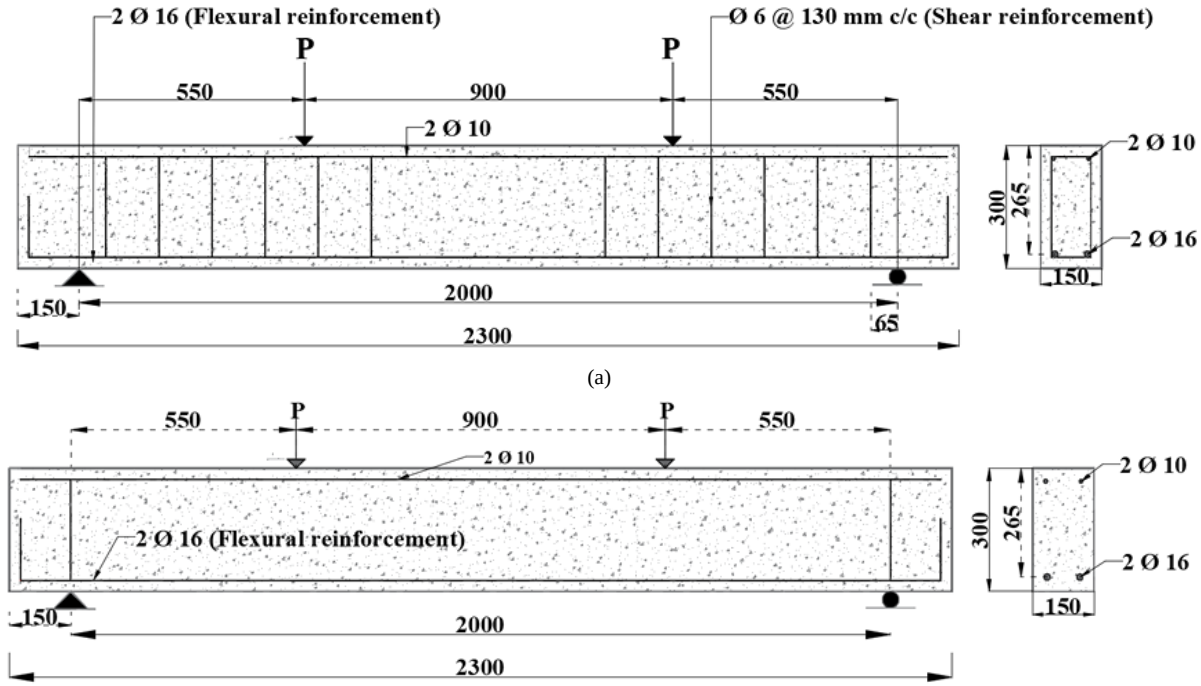

Figure 3. Dimensions and reinforcement details of tested beams (unit: mm): (a) Group S, beams included shear reinforcement in shear span; (b) Group W, beams without any shear reinforcement

The test variables in this study were as follows:

- The amount of shear reinforcement in the critical section (shear span)
- The amount of steel wire mesh layers
- The type of strengthening scheme along the critical shear span: continuous U-jacket, vertical strips, or 45° inclined strips

The nomenclature of the test specimens is labeled using the "$i - X - Y$" format as follows:

The first character refers to the number of wire mesh layers. i takes the value of either 3 or 6.

The second character X denotes the specimen's group. S is used for specimens that had shear stirrups within the shear span, and W is used for specimens without any stirrups.

The third character Y denotes whether the specimen is strengthened with vertical strips (V), continuous U-jacket (UJ) scheme, or inclined strips (K).

The reference specimens were labeled as CS and CW for the specimens with shear stirrups within the shear span and specimens without any stirrups, respectively. Table 2 shows the tested beam specimens.

Table 2. Test variables

No.	Group	Designation	Shear Reinforcement in shear span	Strengthening scheme	Strip orientation	Wire mesh layers
1	S (With Stirrups)	CS	Φ6 mm@130 mm	------	------	------
2		3SUJ		U-Jacket	90°	3
3		6SUJ		U-Jacket	90°	6
4		6SV		U-Strip	90°	6
5		6SK		Sided Strip	45°	6
6	W (Without Stirrups)	CW	-----	------	------	------
7		6WJ		U-Jacket	90°	6
8		6WV		U-Strip	90°	6
9		6WK		Sided Strip	45°	6

A two-component thixotropic epoxy adhesive named "Sikadur-31 CF Slow" that hardens without shrinkage was used to fabricate the WMEC. According to the technical data sheet provided by the manufacturer, after 7 days of curing at 20 °C, the epoxy adhesive will have a tensile adhesion strength greater than 4 MPa, a tensile strength of 13 MPa, a compressive strength of 54 MPa, a flexural strength of 27 MPa, and an elastic modulus of about 2600 MPa.

2.3. Casting and Curing

Plywood molds were utilized as a casting formwork for all concrete beams as shown in Figure 4. All beams were simultaneously cast from one concrete batch. The concrete was mixed using a 5 m3 concrete truck mixer and poured in layers inside the prepared molds. The concrete was carefully compacted inside the forms using a vibrator. The reinforcement steel was separately prepared as cages and positioned inside the forms with proper spacers prior to concrete casting. After casting, the specimens were kept in a humid environment for 24 hours and then demolded. All the specimens were covered with plastic sheets for 28 days. Six concrete cubes, six prisms, and six cylinders were prepared and cured under the same conditions to determine the mechanical properties of the concrete beam specimens.

(a) Molds (b) Casting (c) Vibration Process

(d) Surface Leveling (e) Casted Specimens (f) Demolding

Figure 4. Casting of beam specimens

2.4. Shear Strengthening of Beam Specimens

As mentioned in Section 2.2, the strengthened specimens were divided into three series according to strengthening schemes. The first group includes the beams with six or three layers of wire mesh fabricated with a U-jacket (550 mm in width and 300 mm in depth) and continued along the shear span (Figure 5a). The second group includes strengthened beams with six layers of wire mesh arranged as vertical U-strips (120 mm in width and 300 mm in depth) with 95 mm spacing through the shear span (Figure 5b). The third series included beams that were strengthened with inclined strips with an inclination angle of 45°. The inclined strips had six layers of wire mesh with a width of 70 mm and spacing of

95 mm through the shear span (Figure 5c). For the second and third groups, the strengthening schemes covered about 65% of the critical shear span. The strengthening steps were as follows:

- The wire mesh was cut off to the required dimensions. These fabricated samples were then tied together using fine steel wire to make a single unit and to keep the openings of the successive layers. This step allows the epoxy matrix to easily pass through these layers and ensure good bonding.
- The concrete surface in the shear zone of the beams was graded to remove all sharp edges, loose materials, cement laitance, and contaminants by using an electric grading machine. The surfaces of the specimens were then cleaned using a water jet to remove dust and any other materials that could affect the bonding between the beam surfaces and strengthened materials. The beams' bottom corners were rounded with a radius of curvature of 15 mm, which fulfills the ACI 440.2R-08 [55] minimum requirement (13 mm), to avoid stress concentrations.
- Two small holes of diameter 10 mm were drilled on each side and one on the soffit of the beam for strip and inclined schemes. For the continued scheme, six holes on each side and three on the soffit of the beam were drilled.
- The prepared surfaces were coated with a low-viscosity epoxy primer (Sikafloor-161) [56]. Quartz sand of size 300–600 µm was spread on these surfaces to roughened them and enhance the bonding.
- After the primer layer had hardened, dust was removed using an air blower.
- The fabric of the wire mesh layers was laid in its right position and fixed by inserting a steel screw of 6 mm diameter into the holes.
- The fabric was covered manually by epoxy adhesive. Gentle hand pressure was applied to the epoxy using a spatula tool to guarantee that the epoxy reached the concrete surface. Sikadur-31 [57] was used as an epoxy adhesive. It consists of two components, resin and hardener, which were mixed properly in a ratio of 2:1 by weight using an electric drill at a low speed. Mixing was continued until the components became homogeneous (gray color). The average thickness of the composite for the three and six layers of wire mesh was about 5.5–6.5 and 11–13 mm, respectively. The WMEC was cured at room temperature for at least 7 days before testing to ensure the complete strength of the epoxy resin. Owing to the sensitivity of the mechanical performance of the interface between composite layers and concrete to the workmanship during installation, a similar strengthening procedure was carefully followed for all the members. Prior to the testing day, all the specimens were coated with white color paint to visualize all cracks during the test.

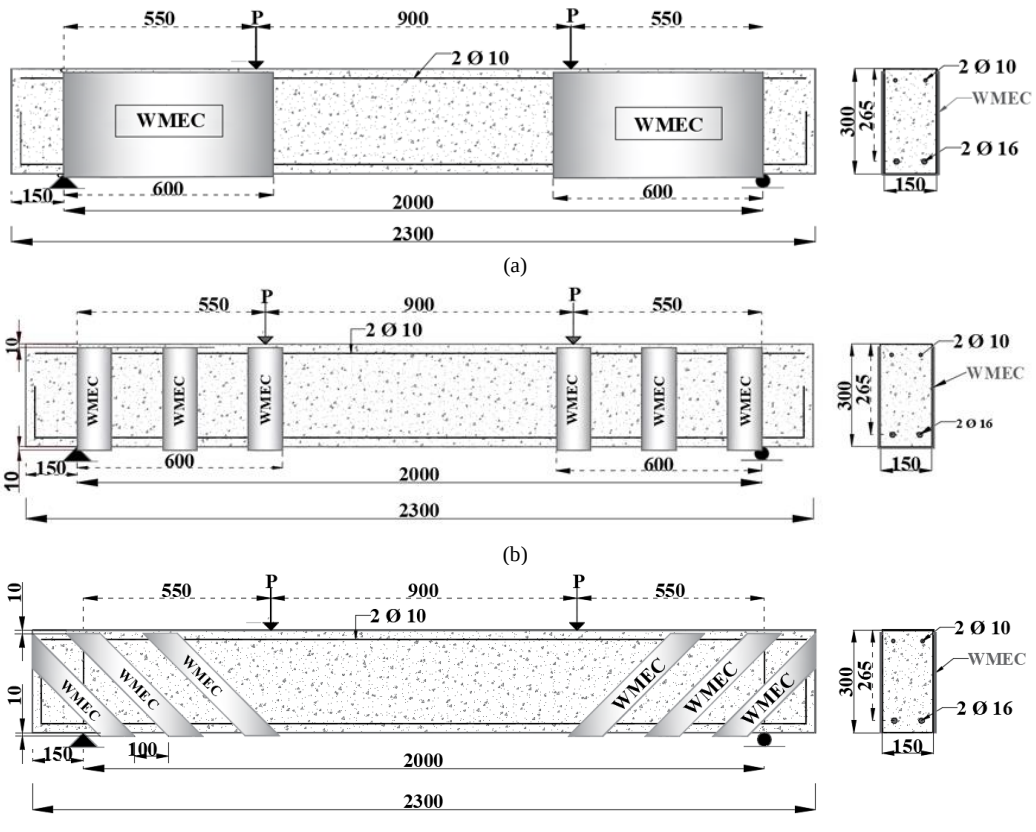

Figure 5. WMEC shear-strengthening schemes (unit in mm): (a) U-jacket strengthening, (b) vertical strip strengthening, and (c) inclined strip strengthening

Figure 6 shows a flowchart for applying WMEC.

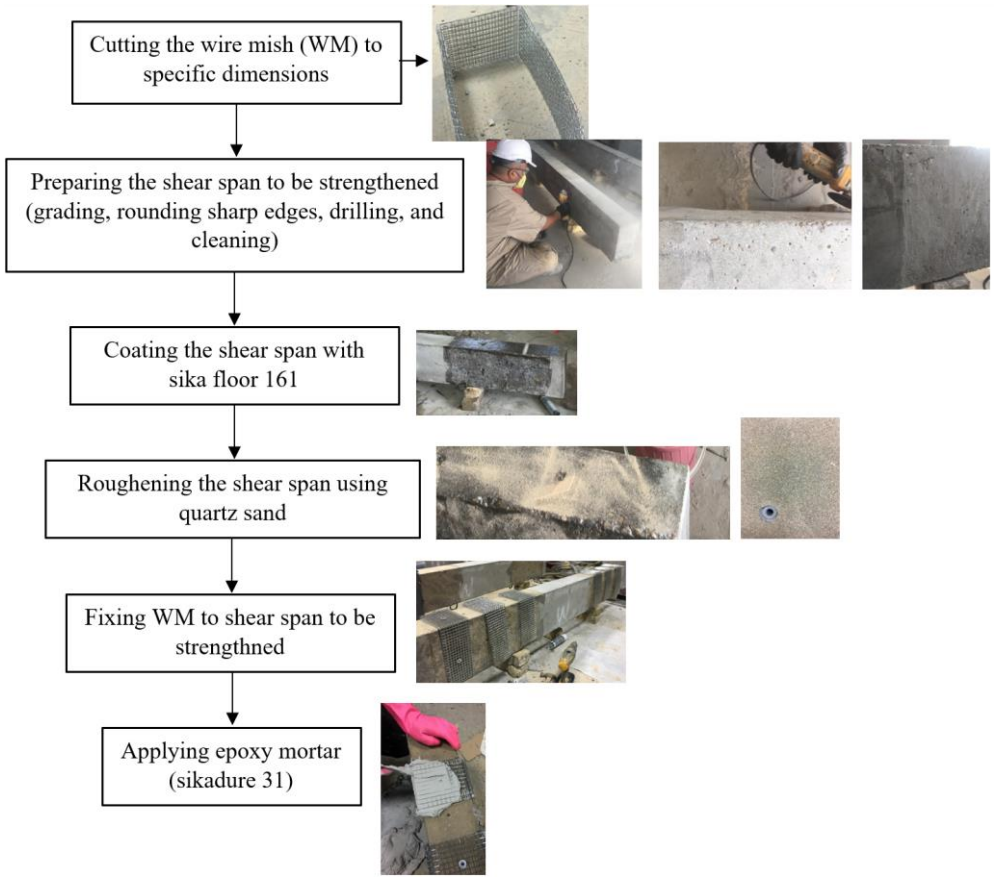

Figure 6. Flowchart for installing WMEC

3. Loading Setup and Instrumentation

All beams were tested under monotonic loading of two points loads (four-point-bending test) with a shear span to effective depth ratio of 2.1. Figure 7 illustrates the arrangement and details of the test setup. The simply supported specimen was placed over the two steel rollers supports at 150 mm from the ends of the beam. The clear span (2000 mm) was divided into three parts: the central part had a 900 mm length between applied forces, and the length of each edge region was 550 mm. A universal testing machine of 600 kN capacity was used to apply the concentrated load on a spreader beam, which then distributed two concentrated loads on the test specimen. The load was monotonically increased in steps up to failure by using a hydraulic load cell of 2.5 kN accuracy. Steel plates and rubber pads were laid above the supports and underneath the loading points to avoid the local crushing of the tested beams. Beam deflection was monitored using two dial gauges of 25 mm capacity with 0.01 division. One was placed at the center of the beam, and the other was placed just below the point of the applied load. Strain gauges were also glued to the concrete surface. Mid-span compressive concrete strain was measured by one electrical strain gauge of 30 mm length and 120 Ω resistance as shown in Figure 7. Instead of a complete strain rosette, one strain gage was installed diagonally because the diagonal strain dominated over the horizontal and vertical strains in the shear span [34]. During the test, a data logger was employed to record and store the test data, which were later transmitted to a computer for further processing. Beam behavior, cracks, and failure modes were recorded throughout the test.

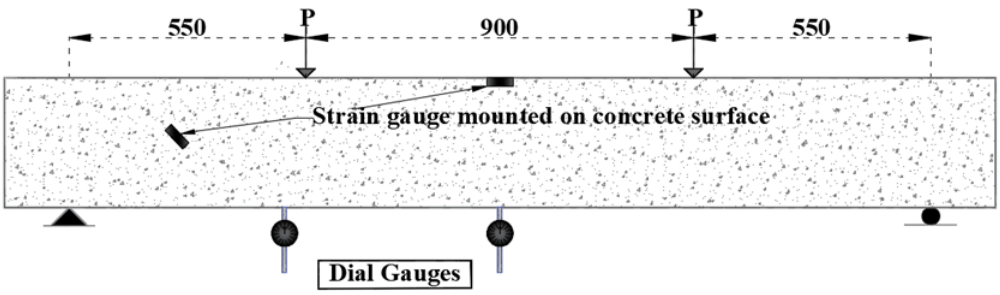

Figure 7. Test setup and instrumentation details

4. Results and Discussion

4.1. Load–Deflection Relationship

The load–midspan deflection relationships for the control beams CW and CS are shown in Figure 8. The behavior of CS and CW is linearly elastic until cracks occur (vertical flexural crack in the central part). With the increase in applied load, shear cracks appear in the shear span zones (edge regions) and the load-deflection relations are changed. One of the inclined shear cracks rapidly widens and extends toward the applied load, thus causing a sudden drop in the applied load. Therefore, the reference beams exhibit brittle failure. CS has higher ultimate load and deflection than CW as shown in Figure 8.

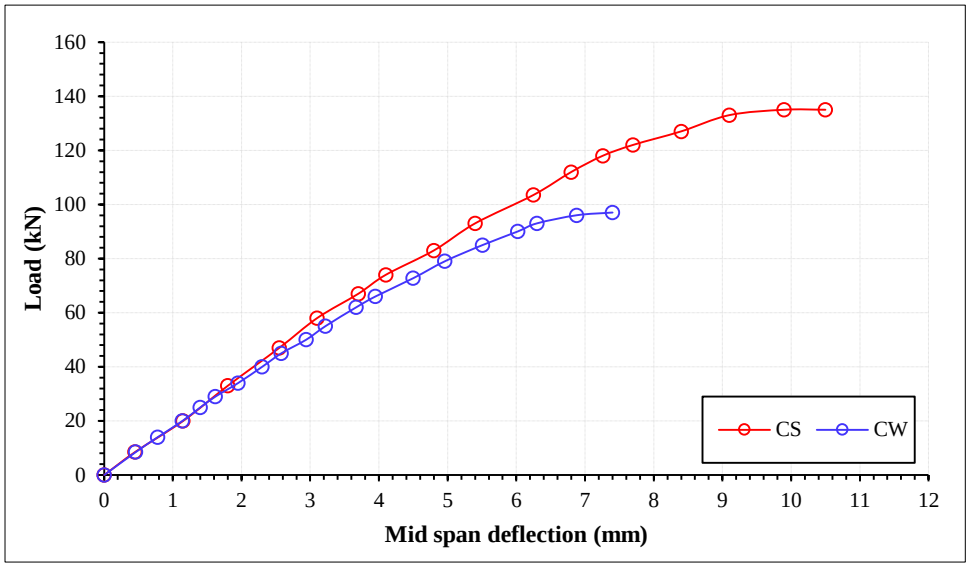

Figure 8. Load–deflection relationships for reference specimens

The load-deflection curves of the strengthened beams (group W and group S) are shown in Figures 9 and 10, respectively. All WMEC-strengthened specimens show flexure behavior, namely, no sudden drop in the load occurs. In general, the final collapse of the strengthened specimens occurs in a ductile manner, that is, their curves are flat near the ultimate load. Initially, the response of the strengthened specimens is similar to that of the reference beams: a linear relationship between load and deflection. With the increase in applied load, the first flexural crack is initiated in the central zone of the specimens, followed by a curve slope change that indicates a reduction in beams' stiffness. Other small flexural cracks then appear in the same region, indicating the yield of steel reinforcements. When the load is close to the ultimate load, shear cracks develop in the shear span zones and the specimen collapses. In this stage, the load–deflection relationships typically become flat with a small increase in the load. All the strengthened specimens exhibit an increase in cracking and ultimate loads compared with the control specimens.

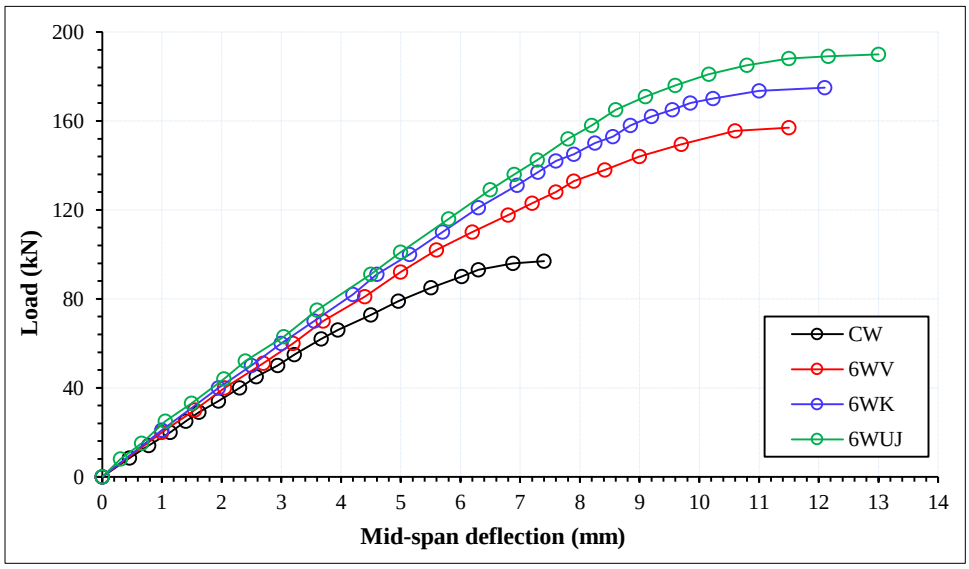

Figure 9. Load–deflection relationships for strengthened specimens without stirrups (group W)

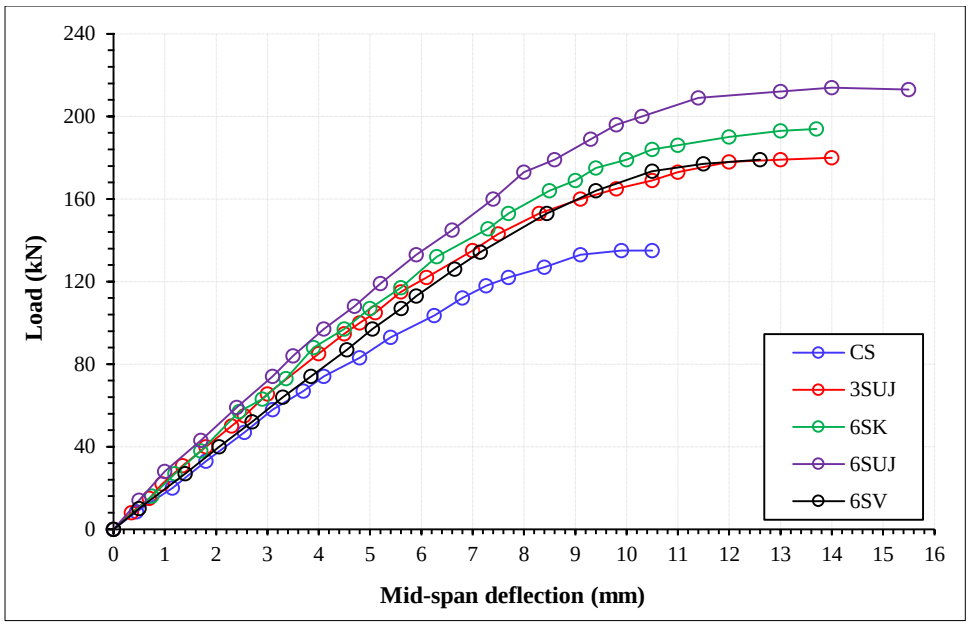

Figure 10. Load–deflection relationships for strengthened specimens with stirrups (group S)

The ultimate load-carrying capacities P_{ult} (failure load) of all tested specimens are listed in Table 3. The P_{ult} of beams strengthened with WMEC is higher than that of the reference beams. For groups S and W, the increase in P_{ult} ranges from 32.6% to 57.8% and from 61.8% to 95.9%, respectively. The WMEC strengthening effect is more in group W than in group S. In group S, the WMEC strengthening system and steel stirrups work together in resisting the shear force, that is, the diagonal tension stresses are repelled from the later loading stages up to the failure stage. For the specimens without shear stirrups, the WMEC strengthening plays a major role in resisting shear forces from the early loading stages up to the failure stage. Group W shows more utilization and benefit of the WMEC strengthening system than group S. Thus, the considerable increase in the P_{ult} of the beams strengthened with WMEC reveals the success of the proposed WMEC technique as a shear-strengthening system.

Table 3. Failure load of beam specimens

No.	Group	Designation	Ultimate Load P_{ult} (kN)	Increase in Ultimate Load (%)
1	S (With Stirrups)	CS	135	-------
2		3SUJ	180	33.4
3		6SUJ	213	57.8
4		6SV	179	32.6
5		6SK	194	43.7
6	W (Without Stirrups)	CW	97	--------
7		6WUJ	190	95.9
8		6WV	157	61.9
9		6WK	175	80.4

The beams strengthened with continuous U-jacket configuration (3SUJ, 6SUJ, and 6WUJ) show a higher increase in P_{ult} than those strengthened with other WMEC configurations that have the same number of wire mesh layers (the P_{ult} of 6SK is 43.7% which is higher than that of 3SUJ). The increase in P_{ult} for specimens 6SUJ and 6WUJ is 57.8% and 95.9%, respectively, and that for beams 6SV and 6WV (specimens that strengthened with vertical strips) is 32.6% and 61.9%, respectively. These results are expected because the continuous U-jacket strengthening configuration involves a large cross-sectional area of the strengthening layer that resists the diagonal tension stresses similarly to the separate vertical strip strengthening configuration. In addition, the large restrained area between WMEC and concrete substrate in the critical regions enhances the shear strength.

In this study, the effect of the wire mesh amount within WMEC was investigated using the continuous U-jacket strengthening pattern in group S. For the continuous U-jacket configuration, the effect of doubling the number of wire mesh layers was studied. The failure loads of beams 3SUJ (3 layers) and 6SUJ (6 layers) are 180 and 213 kN (33.4% and 57.8% increase in P_{ult}), respectively. Therefore, the ultimate load increases by 24.4% when the number of strengthening layers is doubled.

In terms of the orientation of the strengthening patterns, the beams strengthened with inclined strips (45°) show higher load carrying capacities than those strengthened with vertical strips for both groups. For the isolated strip strengthening scheme, the inclination of strips plays an important role in improving the shear strength of the beams. Thus, the increase in P_{ult} for specimen 6SK is 11.1% higher than that for 6SV, and the increase for specimen 6WK is 18.5% higher than that for 6WV. The difference in the ultimate load capacity between these two configurations reaches about 66.7%, although the cross-section area and the amount of wire mesh are almost the same in both cases. This difference is mainly due to the orientation of the wire mesh inside the composite. In the inclined scheme, the orientation of the wire mesh in the composite is almost orthogonal to the crack trajectory. Inclined strengthening prevents the development and propagation of cracks' growth. Therefore, the orientation angle of wire mesh has a significant effect on strength enhancement.

As a result, the increase in the load-carrying capacity of the strengthened beams using WMEC system ranged between 32.6 and 57.8% for the specimens with stirrups in the shear span and between 61.9 and 95.9% for the specimens without stirrups. Therefore, the proposed WMEC systems can effectively improve the load-carrying capacity for all strengthening configurations.

Only the mid-span deflection values were discussed. Mid-span vertical displacement was measured at each load step until failure. The maximum mid-span deflection at the failure load (Δ_{max}) and the ratio of maximum deflection to the deflection of reference beams $\Delta_{max}/\Delta_{ref}$ are presented in Table 4. The $\Delta_{max}/\Delta_{ref}$ ratios are more than unity for all specimens strengthened with WMEC. The ratios of $\Delta_{max}/\Delta_{ref}$ are between 1.2 and 1.48 for group S and between 1.55 and 1.76 for group W. Therefore, the effect of WMEC is highly significant for the beams without shear reinforcement, and this finding is similar to the conclusion on load-carrying capacity. The beams strengthened with continuous U-jacket scheme show higher $\Delta_{max}/\Delta_{ref}$ than those with the other strengthening patterns. In addition, the beams with inclined strip strengthening scheme show higher $\Delta_{max}/\Delta_{ref}$ than those strengthened with the vertical strips. As result, the deformational performance of the specimens without stirrups strengthened with continuous U-jacket is better than those strengthened with discrete or inclined WMEC counterparts.

Table 4. Maximum deflection of tested specimens

No.	Group	Designation	Maximum deflection, mm	$\Delta_{max}/\Delta_{ref}$
1	S (With Stirrups)	CS	10.5	1.00
2		3SUJ	14.0	1.34
3		6SUJ	15.5	1.48
4		6SV	12.6	1.20
5		6SK	13.7	1.31
6	W (Without Stirrups)	CW	7.4	1.00
7		6WUJ	13.0	1.76
8		6WV	11.5	1.55
9		6WK	12.1	1.64

The average $\Delta_{max}/\Delta_{ref}$ for specimens without shear reinforcement is about 24% higher than that for specimens with shear reinforcement. The reference beam without shear reinforcement relies entirely on concrete to provide its shear capacity. Hence, these beams brittlely and suddenly fail without any ductility (Δ_{ref} =7.4 mm). On the contrary, the control beam with internal transverse shear reinforcement has some ductility provided by the stirrups at shear span (Δ_{ref}=10.5 mm). Thus, adding the external strengthening schemes (with good tensile resistance and bonding strength) for both groups has improved the overall ductility of the specimens.

Compared with other studies, the WMEC in the current work considerably improves the shear capacity of RC beams. For groups S and W, the increase in the ultimate load capacity is 32.6%–57.8% and 61.9%–95.9%, respectively. The gain of the load-carrying capacity percentages in this study and other reports are listed in Table 5. In all the mentioned studies, the mode of failure was altered from brittle shear to ductile flexural. The overall dimensions and details of the main and longitudinal reinforcement of the specimens prepared in this study are identical with the specimens prepared by Alam & Riyami [22]. The natural fiber strips were used for strengthening RC beams and bonded into the beam sided (side bonded strips scheme).

Table 5. Comparison of ultimate load gain percentage and deflection ratio

Study	Technique	A gain in shear capacity (%)		$\Delta_{max}/\Delta_{ref}$
		With stirps	Without stirps	
This research	Wire mesh–epoxy composite	32.6–57.8	61.9-95.9	1.2-1.76
Younis et al. [20]	Fabric reinforced cementitious matrix	NA	−9.6–104.0	0.79-2.38
Alam and Al Riyami [11]	Natural fiber-reinforced polymer	10–36	NA	0.52-0.78
Abadel [47]	carbon fiber-reinforced polymer, welled wire mesh, and textile reinforced epoxy mortar	NA	42.5–56.2	0.73-1.43

In comparison, the minimum gain value obtained in the current study of specimen 6SV which has vertical strips is 32.6 % while the gains in the ultimate load of are between (34-36) % and (10-31) % for beams strengthened with untreated and treated natural fibers strips, respectively. The strengthened schemes of the present study are identical with that presented by Younis et al. [20].

Three different materials were used: glass, carbon, and polyphenylene benzobisoxazole (PBO)-FRCM. In the case of using FCRM as full wrapping of shear span, the gains in load were 101.2, 61.4, and 45.5 % for carbon, glass and PBO-FRCM, respectively. In comparison, the gain in the ultimate load of a similar scheme in the current study is 95.9 %. For the inclined strengthening scheme (45 degrees), the gains in load were 45.7, -9.6, and 53.1 % for carbon, glass and PBO-FRCM, respectively. In the current study, the increase of the ultimate load is 80.4% (specimen 6WK). The third configuration of strengthening is U-jacket. The obtained gain for specimen 6WV is 61.9 % while for carbon, glass and PBO-FRCM system were 70.8, 31.7 and 32.4%, respectively. Abadel [47], studied the effect of using different techniques for strengthening shear performance of RC beams. One of these was using welded wire mesh with epoxy mortar as near surface mounted strengthening technique. The gain of ultimate load for specimen BS-WWM tested by Abadel was 56.2 % while it is 61.9 % for specimen 6WV. From the above, it can be concluded that the results of the present study are in accepted range of available provided methods for shear strengthening of RC beams. Also, the proposed technique in this study can represent a promising method for rehabilitation and repairing members prone to shear failure.

In comparison with other researchers, WMEC improves $\Delta_{max}/\Delta_{ref}$. For 6WV, the ration $\Delta_{max}/\Delta_{ref}$=1.55 while it is 1.43 for the specimen BS-WWM [47]. The ratio of maximum deflection of specimens strengthened by natural fibers to the deflection of reference beam conducted by Alam & Al Riyami [22] is less than unity, as shown in Table 5. For the full wrapping system, the ratios $\Delta_{max}/\Delta_{ref}$ were 2.38, 1.88, and 1.65 % for carbon, glass, and PBO-FRCM, respectively [20]. In this study, $\Delta_{max}/\Delta_{ref}$ is 1.76 for specimen 6WUJ. The ratios for the inclined strengthing scheme were 1.47, 0.79, and 1.7 for carbon, glass and PBO-FRCM, respectively [20]. In this study, $\Delta_{max}/\Delta_{ref}$ of 6WK is 1.64. The last configuration of strengthening is U-jacket at intervals. $\Delta_{max}/\Delta_{ref}$ is 1.55 for specimen 6WV, while for carbon, glass, and PBO-FRCM system were 2.32, 1.36, and 1.42, respectively [20]. Thus, it can be concluded that WMEC improves the deflection ratio more than the techniques studied in Alam & Al Riyami [22] and Abadel [47].

4.2. Shear Ductility Index

The performance of structural members subjected to dynamic loads (such as seismic or blast loads) was evaluated according to their ductility. Ductile members can inelastically deform without collapsing. For an RC member, ductility is usually defined as follows:

$$\mu = \frac{\Delta_u}{\Delta_y} \quad (1)$$

where μ is the ductility index, and Δ_y and Δ_u are the yield and ultimate displacements, respectively. In this research, the deflection at yield was calculated using an idealized elastic–plastic curve of the load–deflection diagram as shown in Figure 10. A bilinear curve can be constructed by drawing a straight line from the origin to the point where 75% of the maximum load is on the load–deflection curve [58]. The line is extended so it meets the horizontal line that is tangent to the load–deflection curve at the point of the maximum load.

The shear ductility index of all beams was calculated according to equation 1, and the obtained values are summarized in Table 6. The results show that WMEC strengthening technique improves the beams' shear ductility index. The positive role of this technique in enhancing group W beams' shear ductility index is shown in Table 6.

The amount of wire mesh in the epoxy matrix seems to have an effect on μ. The shear ductility index gain for the jacketing scheme with six layers of wire mesh (6SUJ) is 2.5 times higher than that for the three layers of wire mesh (3SUJ). μ is also sensitive to the WMEC strip inclination. The improvement in shear ductility index caused by the inclined strips is greater than that caused by the vertical strips. In addition, the inclined strips present higher ductility than the vertical strips as shown in Table 6. In comparison to the reference specimen, the deformational behavior of the reinforced beams is generally better. When comparing the continuous U-jacket design of the specimen with stirrups to the reference specimen, the increase in ductility reached 23%.

Table 6. Ductility factor of tested beams

No.	Group	Designation	Yield deflection (mm)	Maximum deflection (mm)	Shear ductility index	Shear ductility Index gain %
1	S	CS	8.20	10.5	1.28	---
2		3SUJ	8.90	14.0	1.57	23
3		6SUJ	9.85	15.5	1.57	23
4		6SV	9.50	12.6	1.33	4
5		6SK	9.70	13.7	1.41	10
6	W	CW	6.00	7.4	1.23	---
7		6WUJ	9.67	13.0	1.34	9
8		6WV	8.77	11.5	1.31	7
9		6WK	9.28	12.0	1.29	5

4.3. Stiffness

Stiffness is an essential factor that affects the serviceability control of members. Thus, the effect of WMEC strengthening technique on beams' stiffness was investigated. Beams' stiffness was calculated by the service load that produces the maximum permissible allowable deflection as defined by ACI 318-14 [54]. The stiffness values of all the tested beams are presented in Table 7. The stiffness of all the strengthened beams is considerably higher than that of the reference specimens. Figures 8 to 10 show that the stiffness of the control and strengthened beams are almost identical until initial cracks appear (linear elastic part of the curve). Beyond cracking development (after the first crack appears), the stiffness of the control specimens decreases, and that of the strengthened members remains unchanged due to the contribution of the strengthening material. L/240 (L is an effective length), i.e., 2000/240= 8.34 mm, is the allowable deflection for roofs or floors constructed as supporting or attached to nonstructural elements that are not likely to be damaged by large deflections. This limitation is considered in determining the stiffness of members. As shown in Table 7, all the strengthened specimens exhibit an increase in stiffness at a service load (the load corresponding to allowable deflection of L/240). The highest increase in stiffness is obtained for the specimens strengthened with continuous U-jackets in both groups. Among the specimens with shear reinforcement, the increase in stiffness for 6SUJ reaches up to 37.96% compared with that for CS. The limiting deflection defined by L/240 (8.34 mm) is higher than the ultimate deflection of control specimen CW (7.4 mm) in group W. This specimen does not contain any shear reinforcement and fails abruptly. Hence, at the service load range for such members, strengthening is crucial to avoid any possible catastrophic shear failure. However, the beams that contain vertical strips (6SV and 6WV) show less improvement in their stiffness.

Table 7. Stiffness and secant modulus stiffness of tested specimens

No.	Group	Designation	Secant Modulus Stiffness (kN/mm)	Secant Modulus Stiffness Gain%	Service load at Δ=L/240 (kN)	Stiffness, at service load (kN/mm)
1	S	CS	16.21	-------	126.8	15.20
2		3SUJ	19.29	19.0	152.4	18.32
3		6SUJ	21.62	33.4	174.9	20.97
4		6SV	18.78	15.9	151.0	18.11
5		6SK	19.93	22.9	161.1	19.32
6	W	CW	16.17	-------	------	------
7		6WUJ	19.55	20.9	159.2	19.09
8		6WV	17.32	7.3	137.0	16.43
9		6WK	18.83	16.5	151.2	18.13

The stiffness of tested beams can also be estimated using the equivalent elastoplastic curve of the load–deflection relationship as shown in Figure 11. In this method, the stiffness of specimens is represented by the secant modulus K_e for the ascending branch of the elastic–plastic curve, which joins the origin point with the point of 0.75 of ultimate load (P = 0.75 Pu) [57]. The values of calculated stiffness of tested specimens in terms of secant modulus are listed in Table 7. The strengthened beams exhibit greater stiffness than the control specimens. For group S, the increase in stiffness is 19, 15.9, 22.9, and 33.4% for 3SUJ, 6SV, 6SK, and 6SUJ, respectively. For group W, the increase in stiffness is 20.9, 7.3, and 16.5% for 6WUJ, 6WV, and 6WK, respectively. This finding illustrates that the WMEC strengthening technique improves the beams' stiffness.

For comparison, the stiffness calculated from the above two methods is presented in Table 7. The variation between these values ranges 2.41–6.64%. Hence, the above calculation methods can be used to estimate the stiffness of strengthened beams with desirable accuracy.

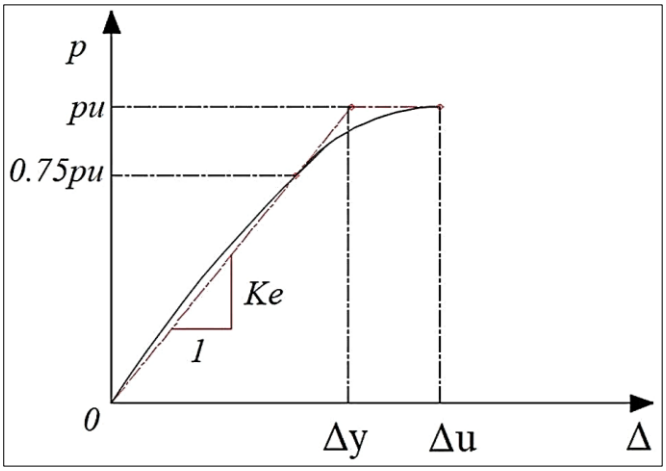

Figure 11. Idealized elastic–plastic curve of the load–deflection diagram

The improvement in strengthened beams' stiffness is due to the contribution of WMEC that restrains the growth of cracks. As mentioned above, the continuous U-jacket configuration significantly improves beams' stiffness compared with the other strengthening configurations due to the large constrained area enclosed by the continuous U scheme along the shear span. For specimens with similar strengthening scheme (continuous U-jacket), 6SUJ has more stiffness than 3SUJ. Thus, the thickness of the strengthened material is another important factor affecting the stiffness (the number of strengthening layers is also important). Doubling the number of strengthening layers using the secant and service load methods improves the stiffness by 14.4% and 17.4%, respectively (specimens 3SUJ and 6SUJ). Shear reinforcement also contributes to the beams' stiffness by limiting the propagation of shear cracks. The stiffness of the specimens in group S is higher than that in group W.

4.4. Energy Absorption

Energy absorption (Ψ) can be estimated as the area under the load–deflection curve up to failure [59]. The values of energy absorption for all the tested beams are summarized in Table 8. For both groups, the energy absorption of the beams strengthened with WMEC is higher than the reference specimens. In group S, the highest energy absorption is reported for beam 6SUJ (2264.42 kN.mm), and the lowest is for the reference beams (880.81 kN.mm). Therefore, the Ψ_{6SUJ}/Ψ_{cs} is about 2.6. In group W, the highest energy absorption is reported for beam 6WUJ (1546.84 kN. mm) and the lowest is for the reference beams (444.82kN.mm). Therefore, the Ψ_{6WUJ}/Ψ_{WC} is about 3.5. The continuous U-jacket technique displayed a better enhancement effect on energy absorption compared with the separated WMEC strips. However, the specimens strengthened with vertical strips, namely, 6SV (1333.17kN.mm) and 6WV (1086.72kN.mm), show minimum increases in energy absorption (see Table 8). The inclined strips exhibit better energy absorption than the vertical strips. The increase in energy absorption is nearly 87% and 185% of the corresponding reference specimens in groups S and W, respectively. The specimens in group W show a higher increase in energy absorption than those in group S as illustrated in Table 8. This increase in the energy absorption of the specimens in group W is due to enhanced stiffness that is contributed by WMEC and delays the failure of the specimens. Therefore, the WMEC technique is relevant to the deformability of the RC members and prevents the abrupt shear failure of strengthened members that occurred in the control specimens. The WMEC-strengthened beams had better energy absorption than the reference specimens, as can be seen in Table 8. For the beams with and without stirrups in the shear span, the specimens strengthened with the continuous U-jacket scheme demonstrated the greatest increase in energy absorption of roughly twice and three times that of the reference specimen, respectively.

Table 8. Energy absorption of tested specimens

No.	Group	Designation	Ultimate Load (kN)	Energy Absorption Ψ, kN.mm	Increase in Energy Absorption, %
1	S	S	135	880.41	-------
2		3SUJ	180	1612.33	83.14
3		6SUJ	205	2264.42	157.20
4		6SV	178	1333.17	51.42
5		6SK	194	1643.21	86.64
6	W	W	97	444.82	------
7		6WUJ	190	1546.84	247.75
8		6WV	157	1086.72	144.31
9		6WK	184	1266.16	184.65

For the continuous full jackets, the gains of energy absorption were 328%, 167% and 116% for carbon, glass and PBO-FRCM, respectively [20], while it is 247.74% for specimen 6WUJ. The gain in ductility for specimen 6WV is 144.31% while in FRCM system of same scheme were 285%, 66.4% and 75% for carbon, glass and PBO-FRCM, respectively. For the inclination scheme, the gain of ductility in specimen 6WK is 184.65 %, whereas they were 96%, -24%, and 130% in carbon, glass, and PBO-FRCM, respectively. It can be concluded that the gain of energy absorption obtained in the present study is higher than that of glass and PBO-FRCM.

4.5. Crack Propagation and Modes of Failure

The reference specimens (CS and CW) show a typical diagonal shear failure mode as illustrated in Figure 12. In the early loading stages, one inclined crack has developed in the shear span zone. With further increase in load, the crack widens and further extends, causing the brittle failure of the beam. The major crack starts near the loading point and extends downward at approximately 45° angle inclination to the support point. Therefore, the failure mode of these beams is a diagonal tension failure that happens due to the splitting of the concrete along the inclined crack at loads of 135 kN and 97 kN for CS and CW, respectively.

(a) Control S specimen

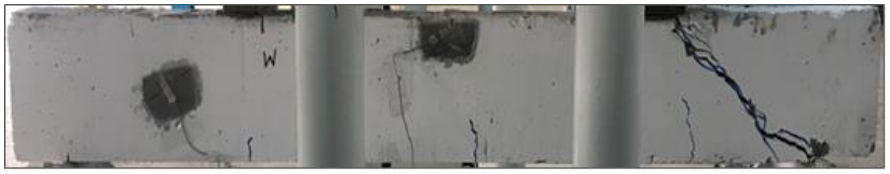

(b) Control W specimen

(c) 3SUJ (jacket specimens)

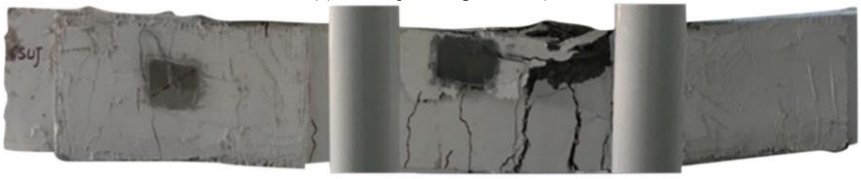

(d) 6SUJ (jacket specimens)

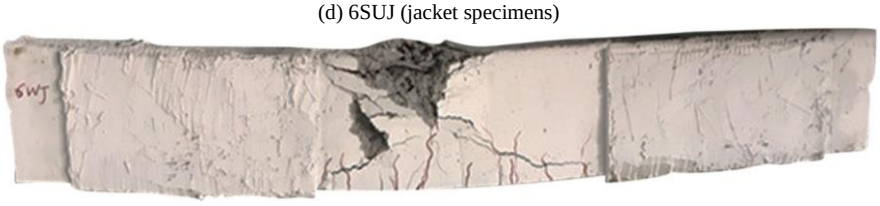

(e) 6WUJ (jacket specimens)

(f) 6SK (strip specimens)

(g) 6WK (strip specimens)

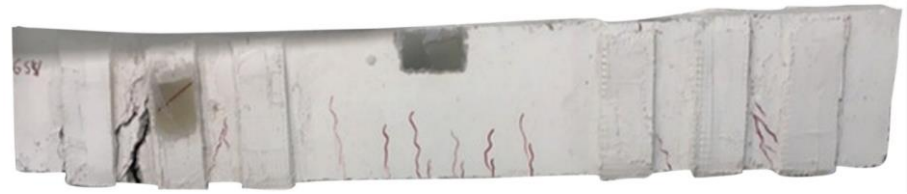

(h) 6SV (strip specimens)

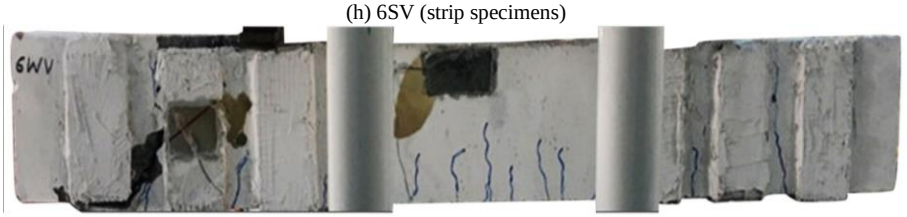

(i) 6WV (strip specimens)

Figure 12. Failure patterns and crack formulation of tested specimens (cont.)

The beams strengthened with the continuous U scheme in both groups show flexural behavior until the failure load. In 3SUJ, 6SUJ, and 6WUJ, the first flexural crack is initiated in the central zone of the specimens (between two applied loads) with the cracking load near 90, 95, and 55 kN, respectively. Beyond this load, the cracks extend toward the top fiber, followed by other small flexural cracks that appear in the same region. The specimen collapses due to the development of one flexural crack in the middle region of the beam, accompanied by the crushing of concrete in the compression zone. The failure loads are 205, 180, and 190 kN for 6SUJ, 3SUJ, and 6WUJ, respectively. The crack patterns at failure are illustrated in Figure 12. During the crushing in the compression zone, the compression reinforcement also buckles as highlighted in Figures 12-c to 12-e. This phenomenon can be attributed to the excellent mechanical properties of WMEC that allow the strengthened beams reach their ultimate strength without debonding or end peelings. The failure of these beams happens in a more ductile fashion compared with the control specimens. The failure modes of the tested beams are listed in Table 9.

Table 9. Failure modes of tested specimens

No.	Group	Designation	Failure mode
1	S (With Stirrups)	CS	Shear
2		3SUJ	Flexure
3		6SUJ	Flexure
4		6SV	Flexure + shear
5		6SK	Flexure + shear
6	W (Without Stirrups)	CW	Shear
7		6WUJ	Flexure
8		6WV	Flexure + shear
9		6WK	Flexure + shear

The failure of the specimens strengthened with vertical and inclined WMEC schemes in both groups (6SK, 6SV, 6WK, and 6WV) were recorded as a combined flexure–shear failure. The failure patterns of the specimens at the collapse stage are shown in Figure 12. With the increase in load, many flexural cracks appear between the points of applied loads. The first flexural cracking starts at loads of 60, 90, 40, and 50 kN for 6SV, 6SK, 6WV, and 6WK, respectively. Beyond this load, cracks extend toward the top fiber, and additional flexural cracks have developed throughout the beam length. Inclined cracks later appear in both shear span zones close to the beam supports. The inclination angle of these cracks ranges between 35° and 45°. Increasing the load causes damage to the enclosed region between the load points and a 120 mm distance from the support. This phenomenon continues until the WMEC strips break heavily (Figures 12-f to 21-i). Failure occurs at loads of 178, 194, 154, and 184 kN for 6SV, 6SK, 6WV, and 6WK, respectively. In this stage, the beam could not endure any further load, and deformation continues due to sequestration supplied by the WMEC strips. The beams behave in a ductile manner until the jacket strips have fractured on both sides of the beams.

No detachment at the interface between the concrete substrate and WMEC system and/or between the epoxy and wire meshes is observed for all the strengthened specimens. The removal of the jacket strips reveals that the WMEC has an excellent attachment to the concrete substrate, and no debonding occurs between them. The test of the strengthened specimens reveals the influence of WMEC on the breakdown situation and the formation and development of cracks. Owing to this enhancing role for the shear capacity of the beams, this system may be deemed as an alternative to shear reinforcement or a solution for beams suffering defects in shear capacity. Thus, the cracking patterns and modes of failure for the WMEC-strengthened beams are dominated by the WMEC configuration.

4.6. Strain Results

The strains in the concrete were measured using two strain gauges. The first gauge is a 45° strain gauge along the critical shear span at the mid-height of the beam that was used to measure the maximum WMEC tensile strain. The second strain gauge was placed at the top compression region at the beam's mid-span. WMEC strain is a reasonable indication of the concrete strain. The diagonal tensile strain and top compressive strain reading at the failure of each specimen are summarized in Table 10 and shown in Figures 13 and 14 for groups S and W, respectively.

Table 10. Maximum strains at the failure load of tested specimens

No.	Group	Designation	Ultimate Load (2P), kN	Max. Diagonal Strain	Max. Comp. Flexural Strain
1	S	CS	135	0.001012	0.002001
2		3SUJ	180	0.001338	0.001593
3		6SUJ	205	0.001547	0.001392
4		6SV	178	0.001569	0.001011
5		6SK	194	0.001005	0.001973
6	W	CW	97	0.000052	0.000744
7		6WUJ	190	0.001035	0.002328
8		6WV	157	0.003656	0.002025
9		6WK	184	0.000935	0.001957

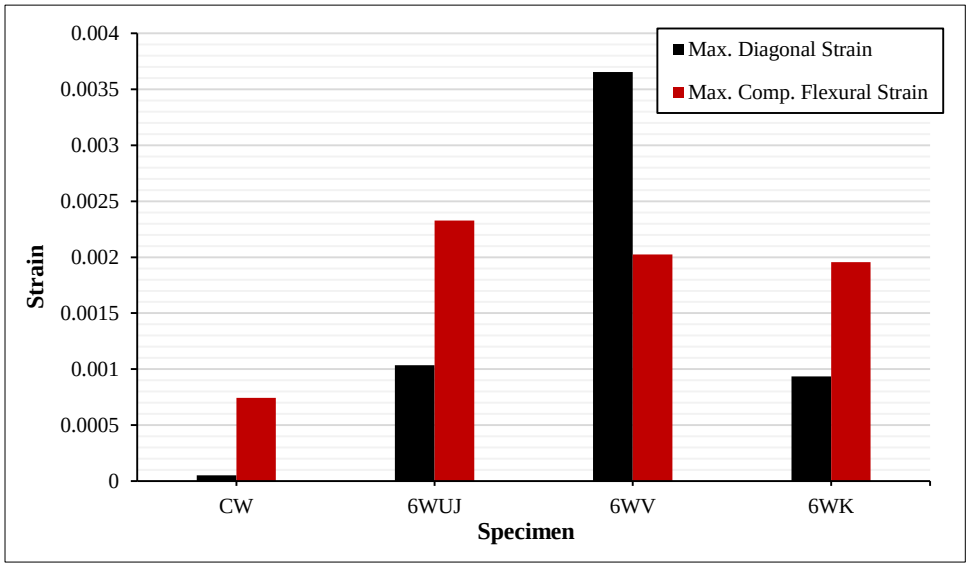

Figure 13. Strains at the failure load of Group W

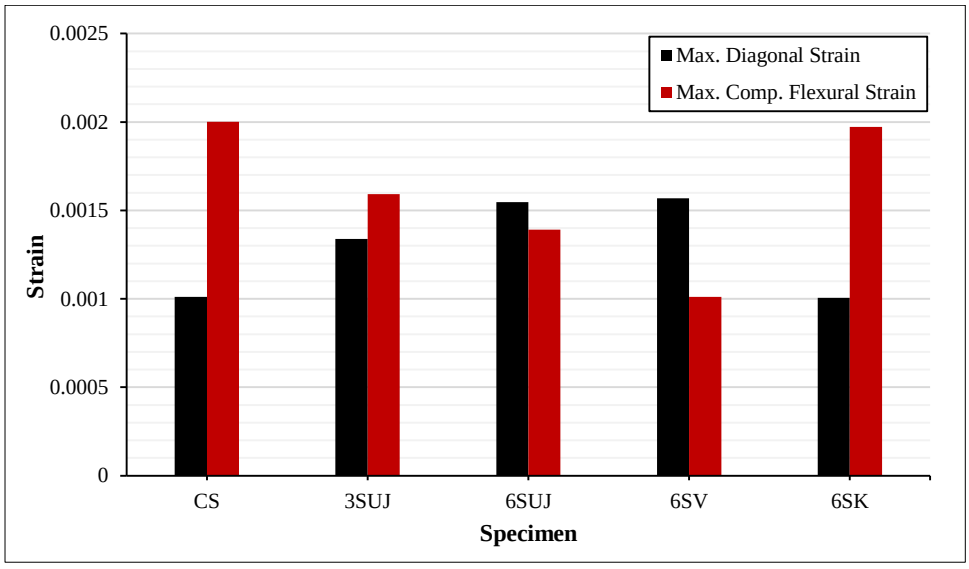

Figure 14. Strains at the failure load of Group S

According to Figure 13 (group W), the maximum diagonal and compressive strains at the failure for all strengthened specimens are significantly greater than those for CW. This finding indicates the positive impact of the WMEC strengthening system in delaying brittle shear failure. Upon failure, 6WV and 6WK show similar flexural compressive strains, indicating their shear failure. In addition, the tensile diagonal strain values of 6WJ and 6WK are close to each other and lower than the diagonal strain of 6WV. However, the failure loads of 6WJ and 6WK are higher than that of 6WV. This finding indicates the better performance of the inclined strips and U-jacket configuration compared with the vertical strips.

According to Figure 14 (group S), the flexural compressive strains at the failure for all specimens are lower than those for the control beams. In particular, 3SUJ and 6SK yield lower tensile diagonal strains than the control and other beams. 6SV has relatively low compressive strain and high tensile diagonal strain, indicating its shear failure. Therefore, the performance of the vertical strip configuration is poorer than that of the other strengthening schemes. In addition, all the beams have greater tensile diagonal strain than the control specimen, except for 6SK, which has a close strain value to the control beam. For comparison, the strain states of group S specimens and the strains at the load of 135 kN (the failure of control specimen CS) were computed and are presented in Figure 15. The compressive strains for all strengthened specimens are lower than those for the control specimen.

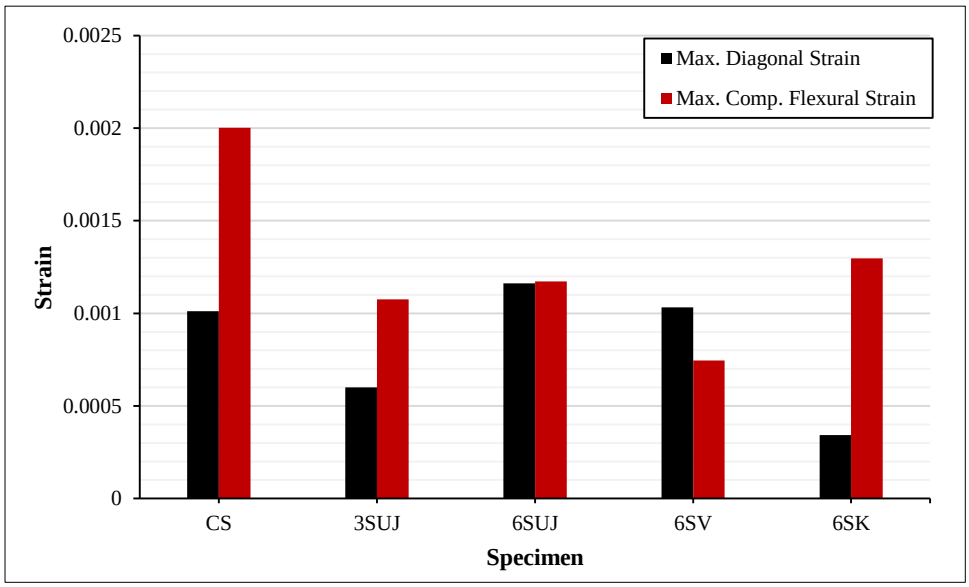

Figure 15. Compressive strains at a load of 135 kN

5. Conclusions

The effectiveness of WMEC as a shear-strengthening technique for RC beams was investigated by testing nine rectangular cross-section beams with and without stirrups within the shear span. The following conclusions can be drawn:

- The proposed WMEC systems effectively improve the load-carrying capacity. Compared with the non-strengthened reference beams (for different strengthening schemes), the increase in the load-carrying capacity of the strengthened beams ranged between 32.6% and 57.8% for the specimens with stirrups in the shear span and between 61.9% and 95.9% for the specimens without stirrups.
- The deformational behavior of the strengthened beams was generally improved relative to that of the reference specimen. Compared to the reference specimen, the continuous U-jacket scheme of the specimen with stirrups in the shear span increased ductility by 23%.
- The effect of WMEC strengthening increased with the number of steel wire mesh layers inside the WMEC. The beam with six layers of wire mesh increased the ultimate load to 57.8%, which was higher than the 33.4% provided by three layers. The load-carrying capacity increased by about 72% when the number of layers was doubled.
- The WMEC strengthened pattern had an essential effect on the failure mode and load capacity of beams. The continuous U-jacket configuration was the best pattern for improving the beam performance.
- The WMEC systems increased the beams' stiffness and reduced deflection compared with the control specimens. The increase in the stiffness of the strengthened beams (for different strengthening schemes) ranged from 19.8% to 31.4% for the specimens with stirrups in shear span and from 40% to 60% for the specimens without stirrups.

- All the WMEC-strengthened beams showed higher energy absorption than the reference specimens. The specimens strengthened with a continuous U-jacket scheme showed the maximum increase in energy absorption of about twice and three times that of the reference specimen for the beams with and without stirrups in the shear span, respectively.
- The WMEC-strengthened beams generally yielded two types of failure modes: flexural failure for the continuous U-jacket scheme and flexural–shear failure for vertical and inclined strip schemes. Both control beams failed in diagonal tension failure mode. Thus, WMEC efficiently transformed the failure into flexural.
- WMEC improves beams' deflection, load-carrying capacity, and energy absorption better than other strengthening techniques such as natural fiber-reinforced polymer, glass, and PBO-FRCM.

In summary, the proposed WMEC technique is an effective method to improve the shear strength of RC beams and is suitable for practical application in rapid strengthening. Further studies using different types of wire mesh and shapes are recommended. Also, WMEC can be tested for strengthening other concrete structural members, such as deep beams.

6. Declarations

6.1. Author Contributions

Conceptualization, M.A.B., A.J., H.H., and A.D.; methodology, M.A.B., and A.J.; writing—original draft preparation, M.A.B., and A.J.; writing—review and editing, H.H., and A.D. All authors have read and agreed to the published version of the manuscript.

6.2. Data Availability Statement

The data presented in this study are available in article.

6.3. Funding

The authors received no financial support for the research, authorship, and/or publication of this article.

6.4. Acknowledgements

The authors are grateful to the Department of Civil Engineering, College of Engineering, the University of Misan for the support.

6.5. Conflicts of Interest

The authors declare no conflict of interest.

7. References

[1] Thanoon, W. A., Jaafar, M. S., Kadir, M. R. A., & Noorzaei, J. (2005). Repair and structural performance of initially cracked reinforced concrete slabs. Construction and Building Materials, 19(8), 595–603. doi:10.1016/j.conbuildmat.2005.01.011.

[2] Barnes, R. A., Baglin, P. S., Mays, G. C., & Subedi, N. K. (2001). External steel plate system for the shear strengthening of reinforced concrete beams. Engineering Structures, 23(9), 1162–1176. doi:10.1016/S0141-0296(00)00124-3.

[3] Adhikary, B. B., Mutsuyoshi, H., & Sano, M. (2000). Shear strengthening of reinforced concrete beams using steel plates bonded on beam web: Experiments and analysis. Construction and Building Materials, 14(5), 237–244. doi:10.1016/S0950-0618(00)00023-4.

[4] Abdalla, J. A., Abu-Obeidah, A. S., Hawileh, R. A., & Rasheed, H. A. (2016). Shear strengthening of reinforced concrete beams using externally-bonded aluminum alloy plates: An experimental study. Construction and Building Materials, 128, 24–37. doi:10.1016/j.conbuildmat.2016.10.071.

[5] Li, W., & Leung, C. K. Y. (2017). Effect of shear span-depth ratio on mechanical performance of RC beams strengthened in shear with U-wrapping FRP strips. Composite Structures, 177, 141–157. doi:10.1016/j.compstruct.2017.06.059.

[6] Oller, E., Pujol, M., & Marí, A. (2019). Contribution of externally bonded FRP shear reinforcement to the shear strength of RC beams. Composites Part B: Engineering, 164, 235–248. doi:10.1016/j.compositesb.2018.11.065.

[7] Lee, D. H., Han, S. J., Kim, K. S., & LaFave, J. M. (2017). Shear strength of reinforced concrete beams strengthened in shear using externally-bonded FRP composites. Composite Structures, 173, 177–187. doi:10.1016/j.compstruct.2017.04.025.

[8] Baghi, H., Barros, J. A. O., & Rezazadeh, M. (2017). Shear strengthening of damaged reinforced concrete beams with Hybrid Composite Plates. Composite Structures, 178, 353–371. doi:10.1016/j.compstruct.2017.07.039.

[9] Baghi, H., Barros, J. A. O., & Menkulasi, F. (2016). Shear strengthening of reinforced concrete beams with Hybrid Composite Plates (HCP) technique: Experimental research and analytical model. Engineering Structures, 125, 504–520. doi:10.1016/j.engstruct.2016.07.023.

[10] Lourenço, L., Zamanzadeh, Z., Barros, J. A. O., & Rezazadeh, M. (2018). Shear strengthening of RC beams with thin panels of mortar reinforced with recycled steel fibres. Journal of Cleaner Production, 194, 112–126. doi:10.1016/j.jclepro.2018.05.096.

[11] Alam, M. A., & Al Riyami, K. (2018). Shear strengthening of reinforced concrete beam using natural fibre reinforced polymer laminates. Construction and Building Materials, 162, 683–696. doi:10.1016/j.conbuildmat.2017.12.011.

[12] Shomali, A., Mostofinejad, D., & Esfahani, M. R. (2020). Effective strain of CFRP in RC beams strengthened in shear with NSM reinforcements. Structures, 23, 635–645. doi:10.1016/j.istruc.2019.10.020.

[13] Jalali, M., Sharbatdar, M. K., Chen, J. F., & Jandaghi Alaee, F. (2012). Shear strengthening of RC beams using innovative manually made NSM FRP bars. Construction and Building Materials, 36, 990–1000. doi:10.1016/j.conbuildmat.2012.06.068.

[14] Shomali, A., Mostofinejad, D., & Esfahani, M. R. (2021). Shear strengthening of RC beams using EBRIG CFRP strips: a comparative study. European Journal of Environmental and Civil Engineering, 25(14), 2540–2556. doi:10.1080/19648189.2019.1633413.

[15] Lu, X. Z., Teng, J. G., Ye, L. P., & Jiang, J. J. (2005). Bond-slip models for FRP sheets/plates bonded to concrete. Engineering Structures, 27(6), 920–937. doi:10.1016/j.engstruct.2005.01.014.

[16] Ceroni, F., Pecce, M., Bilotta, A., & Nigro, E. (2012). Bond behavior of FRP NSM systems in concrete elements. Composites Part B: Engineering, 43(2), 99–109. doi:10.1016/j.compositesb.2011.10.017.

[17] Alwash, D., Kalfat, R., Al-Mahaidi, R., & Du, H. (2021). Shear strengthening of RC beams using NSM CFRP bonded using cement-based adhesive. Construction and Building Materials, 301, 124365. doi:10.1016/j.conbuildmat.2021.124365.

[18] Al-Rousan, R. Z., & Shannag, M. J. (2018). Shear Repairing and Strengthening of Reinforced Concrete Beams Using SIFCON. Structures, 14, 389–399. doi:10.1016/j.istruc.2018.05.001.

[19] Meda, A., Mostosi, S., & Riva, P. (2014). Shear strengthening of reinforced concrete beam with high-performance fiber-reinforced cementitious composite jacketing. ACI Structural Journal, 111(5), 1059–1068. doi:10.14359/51686807.

[20] Younis, A., Ebead, U., & Shrestha, K. C. (2017). Different FRCM systems for shear-strengthening of reinforced concrete beams. Construction and Building Materials, 153, 514–526. doi:10.1016/j.conbuildmat.2017.07.132.

[21] Tetta, Z. C., Triantafillou, T. C., & Bournas, D. A. (2018). On the design of shear-strengthened RC members through the use of textile reinforced mortar overlays. Composites Part B: Engineering, 147, 178–196. doi:10.1016/j.compositesb.2018.04.008.

[22] Tzoura, E., & Triantafillou, T. C. (2014). Shear strengthening of reinforced concrete T-beams under cyclic loading with TRM or FRP jackets. Materials and Structures, 49(1-2), 17–28. doi:10.1617/s11527-014-0470-9.

[23] Contamine, R., Si Larbi, A., & Hamelin, P. (2013). Identifying the contributing mechanisms of textile reinforced concrete (TRC) in the case of shear repairing damaged and reinforced concrete beams. Engineering Structures, 46, 447–458. doi:10.1016/j.engstruct.2012.07.024.

[24] Tetta, Z. C., Koutas, L. N., & Bournas, D. A. (2015). Textile-reinforced mortar (TRM) versus fiber-reinforced polymers (FRP) in shear strengthening of concrete beams. Composites Part B: Engineering, 77, 338–348. doi:10.1016/j.compositesb.2015.03.055.

[25] Awani, O., El-Maaddawy, T., & El Refai, A. (2016). Numerical Simulation and Experimental Testing of Concrete Beams Strengthened in Shear with Fabric-Reinforced Cementitious Matrix. Journal of Composites for Construction, 20(6), 4016056. doi:10.1061/(asce)cc.1943-5614.0000711.

[26] Contamine, R., Si Larbi, A., & Hamelin, P. (2013). Identifying the contributing mechanisms of textile reinforced concrete (TRC) in the case of shear repairing damaged and reinforced concrete beams. Engineering Structures, 46, 447–458. doi:10.1016/j.engstruct.2012.07.024.

[27] Chen, C., Yang, Y., Zhou, Y., Xue, C., Chen, X., Wu, H., ... & Li, X. (2020). Comparative analysis of natural fiber reinforced polymer and carbon fiber reinforced polymer in strengthening of reinforced concrete beams. *Journal of cleaner production*, *263*, 121572. doi:10.1016/j.jclepro.2020.121572.

[28] Escrig, C., Gil, L., Bernat-Maso, E., & Puigvert, F. (2015). Experimental and analytical study of reinforced concrete beams shear strengthened with different types of textile-reinforced mortar. Construction and Building Materials, 83, 248–260. doi:10.1016/j.conbuildmat.2015.03.013.

[29] Triantafillou, T. C., & Papanicolaou, C. G. (2006). Shear strengthening of reinforced concrete members with textile reinforced mortar (TRM) jackets. Materials and Structures, 39(1), 93–103. doi:10.1617/s11527-005-9034-3.

[30] Trapko, T., Urbańska, D., & Kamiński, M. (2015). Shear strengthening of reinforced concrete beams with PBO-FRCM composites. Composites Part B: Engineering, 80, 63–72. doi:10.1016/j.compositesb.2015.05.024.

[31] Tetta, Z. C., Koutas, L. N., & Bournas, D. A. (2015). Textile-reinforced mortar (TRM) versus fiber-reinforced polymers (FRP) in shear strengthening of concrete beams. Composites Part B: Engineering, 77, 338–348. doi:10.1016/j.compositesb.2015.03.055.

[32] Kotynia, R., Oller, E., Marí, A., & Kaszubska, M. (2021). Efficiency of shear strengthening of RC beams with externally bonded FRP materials – State-of-the-art in the experimental tests. Composite Structures, 267, 113891. doi:10.1016/j.compstruct.2021.113891.

[33] Amran, Y. M., Alyousef, R., Alabduljabbar, H., & El-Zeadani, M. (2020). Clean production and properties of geopolymer concrete; A review. Journal of Cleaner Production, 251, 119679. doi:10.1016/j.jclepro.2019.119679.

[34] Tetta, Z. C., Koutas, L. N., & Bournas, D. A. (2016). Shear strengthening of full-scale RC T-beams using textile-reinforced mortar and textile-based anchors. Composites Part B: Engineering, 95, 225–239. doi:10.1016/j.compositesb.2016.03.076.

[35] Awani, O., El-Maaddawy, T., & El Refai, A. (2016). Numerical Simulation and Experimental Testing of Concrete Beams Strengthened in Shear with Fabric-Reinforced Cementitious Matrix. Journal of Composites for Construction, 20(6). doi:10.1061/(asce)cc.1943-5614.0000711.

[36] Ombres, L., & Verre, S. (2021). Shear strengthening of reinforced concrete beams with SRG (Steel Reinforced Grout) composites: Experimental investigation and modelling. Journal of Building Engineering, 42, 103047. doi:10.1016/j.jobe.2021.103047.

[37] Gonzalez-Libreros, J. H., Sneed, L. H., D'Antino, T., & Pellegrino, C. (2017). Behavior of RC beams strengthened in shear with FRP and FRCM composites. Engineering Structures, 150, 830–842. doi:10.1016/j.engstruct.2017.07.084.

[38] Ombres, L., & Verre, S. (2019). Flexural Strengthening of RC Beams with Steel-Reinforced Grout: Experimental and Numerical Investigation. Journal of Composites for Construction, 23(5). doi:10.1061/(asce)cc.1943-5614.0000960.

[39] Paramasivam, P., Lim, C. T. E., & Ong, K. C. G. (1998). Strengthening of RC beams with ferrocement laminates. Cement and Concrete Composites, 20(1), 53–65. doi:10.1016/S0958-9465(97)00068-1.

[40] Shebl, H., & El-Nemr, A. (2021). Moment Redistribution of Shear-Critical GFRP Reinforced Continuously Supported Slender Beams. Civil Engineering Journal, 7, 13-31. doi:10.28991/CEJ-SP2021-07-02.

[41] Yan, M. (2015). High toughness resin concrete with steel wire mesh and the reinforcement theoretical research on prestressed concrete simply supported plate beam bridge. Southwest Jiaotong University, Chengdu, China.

[42] Li, X., Xie, H., Yan, M., Gou, H., Zhao, G., & Bao, Y. (2018). Eccentric compressive behavior of reinforced concrete columns strengthened using steel mesh reinforced resin concrete. Applied Sciences (Switzerland), 8(10). doi:10.3390/app8101827.

[43] Qeshta, I. M. I., Shafigh, P., Jumaat, M. Z., Abdulla, A. I., Ibrahim, Z., & Alengaram, U. J. (2014). The use of wire mesh-epoxy composite for enhancing the flexural performance of concrete beams. Materials and Design, 60, 250–259. doi:10.1016/j.matdes.2014.03.075.

[44] Qeshta, I. M. I., Shafigh, P., Jumaat, M. Z., Abdulla, A. I., Alengaram, U. J., & Ibrahim, Z. (2014). Flexural behaviour of concrete beams bonded with wire mesh-epoxy composite. Applied Mechanics and Materials, 567, 411–416. doi:10.4028/www.scientific.net/AMM.567.411.

[45] Jaafer, A. A., AL-Shadidi, R., & Kareem, S. L. (2019). Enhancing the punching load capacity of reinforced concrete slabs using an external epoxy-steel wire mesh composite. Fibers, 7(8), 68. doi:10.3390/fib7080068.

[46] Al Nuaimi, N., Sohail, M. G., Hawileh, R. A., Abdalla, J. A., & Douier, K. (2020). Durability of reinforced concrete beams strengthened by galvanized steel mesh-epoxy systems under harsh environmental conditions. Composite Structures, 249, 112547. doi:10.1016/j.compstruct.2020.112547.

[47] Abadel, A. A. (2021). Experimental investigation for shear strengthening of reinforced self-compacting concrete beams using different strengthening schemes. Journal of Materials Research and Technology, 15, 1815–1829. doi:10.1016/j.jmrt.2021.09.012.

[48] ASTM C33-03. (2010). Standard Specification for Concrete Aggregates. ASTM International, Pennsylvania, United States. doi:10.1520/C0033-03.

[49] BS 1881-116. (1983). Part 116: Method for Determination of Compressive Strength of Concrete Cubes. British Standards Institution, London, Unite Kingdom.

[50] ASTM C78-09. (2010). Standard Test Method for Flexural Strength of Concrete (Using Simple Beam with Third-Point Loading). ASTM International, Pennsylvania, United States. doi:10.1520/C0078-09.

[51] ASTM C496-96. (2010). Standard Test Method for Splitting Tensile Strength of Cylindrical Concrete Specimens. ASTM International, Pennsylvania, United States. doi:10.1520/C0496-96.

[52] ASTM A615/A615-04. (2017). Standard Specification for Deformed and Plain Carbon-Steel Bars for Concrete Reinforcement. ASTM International, Pennsylvania, United States. doi:10.1520/A0615-A0615M-04.

[53] ACI 549.1 R-88. (1988). Guide for the Design, Construction, and Repair of Ferrocement. ACI Structural Journal, 85(3), 32-51.

[54] ACI Code 318-19. (2019). Building Code Requirements for Structural Concrete. American Concrete Institute, Farmington Hills, United States. doi:10.14359/51716937.

[55] ACI 440.2R-08. (2008). Guide for the Design and Construction of Externally Bonded FRP Systems for Strengthening Concrete Structures. American Concrete Institute, Farmington Hills, United States.

[56] Sikafloor®-161. (2016). Product Data sheet. 2-Part Epoxy Primer, Levelling Mortar and Intermediate Layer. Building Trust, Sika. Available online: https://gcc.sika.com/content/dam/dms/gcc/s/sikafloor_-161.pdf (accessed on May 2022).

[57] Sikadur®-31. (2016). CF-Slow: Product Data sheet. 2-Component Thixotropic Epoxy Adhesive. Available online: https://egy.sika.com/content/dam/dms/eg01/g/sikadur_-31_cf_slow.pdf (accessed on May 2022).

[58] Liu, X., Chen, Y., Li, L. Z., Su, M. N., Lu, Z. D., & Yu, K. Q. (2019). Experimental study on the shear performance of reinforced concrete beams strengthened with bolted side-plating. Sustainability (Switzerland), 11(9). doi:10.3390/su11092465.

[59] Ebead, U., Shrestha, K. C., Afzal, M. S., El Refai, A., & Nanni, A. (2017). Effectiveness of Fabric-Reinforced Cementitious Matrix in Strengthening Reinforced Concrete Beams. Journal of Composites for Construction, 21(2), 4016084. doi:10.1061/(asce)cc.1943-5614.0000741.